Journal of Environmental Chemical Engineering 6 (2018) 404–415

Contents lists available at ScienceDirect

Journal of Environmental Chemical Engineering

journal homepage: www.elsevier.com/locate/jece

Thermal decomposition under oxidative atmosphere of lignocellulosic wastes: Different kinetic methods application

Anabel Fernandez[a], German Mazza[b], Rosa Rodriguez[a,*]

[a] Instituto de Ingeniería Química, Facultad de Ingeniería, Universidad Nacional de San Juan, Libertador 1109 (O), San Juan, Argentina
[b] Instituto de Investigación y Desarrollo en Ingeniería de Procesos, Biotecnología y Energías Alternativas, CONICET-Universidad Nacional del Comahue, Neuquén, Argentina

ARTICLE INFO

Keyword:
Lignocellulosic wastes
Combustion
Kinetic behaviour
Thermogravimetric analysis
Isoconversional and non-isoconversional methods
Thermodynamic parameters

ABSTRACT

Combustion of six lignocellulosic wastes was studied using thermogravimetric analysis. Experimental data were analyzed using different kinetic methods Kissinger, FWO, DAEM linear multiple regression methods and Coast Redfern method. Also, their thermodynamic parameters (ΔG, ΔH, ΔS) were obtained.

The activation energy (E) and the pre-exponential factor (A) values calculated by the DAEM, FWO and Kissinger methods were higher than those obtained by the linear multiple regression and Coast Redfern methods. The E values obtained from the Kissinger method are consistent with the range of values obtained by the FWO and DAEM methods and are very near to their average values (between 52.75 and 116.92 kJ/mol for all studied agro-industrial wastes). DAEM and FWO methods provides E and A distributions, detecting multi-step kinetics. However, Kissinger method provides only one E and A values for all heating rates, similar to obtained values applying DAEM and FWO methods.

The linear multiple regression method provides the knowledge of kinetic triplets for each studied heating rate, presenting a slower fit than the other methods. On the other hand, Coast Redfern method supplies these triplets and the reaction mechanisms. However, using this method, the obtained E values are very different to the calculated values applying isoconversional methods. Using the last mentioned methods, the models of volume contraction and first order describe the devolatilization and char combustion stages, respectively.

The obtained thermodynamic parameters values show that the lignocellulosic wastes combustion has a low reaction favorability.

1. Introduction

In past decades, fossil fuel reserves are continuously depleting, and they also adversely affect the environment. Due to these concerns, significant efforts are directed globally to search for alternate renewable energy and environment friendly fuel sources. Among different types of biomass, lignocellulosic biomass has emerged as an attractive source for producing liquid fuels due to its low cost and abundance.

Due to the high variety of raw materials, the processes to transform biomass in energy are numerous. Between these processes, pyrolysis, gasification or combustion are a good solution for technical application. Considering the combustion, it is a chemically complex process in which several reactions occur simultaneously, depending on the operating conditions.

Knowledge of the chemical composition, the thermal behavior during combustion, is very important for the effective design and operation of the thermochemical conversion units. Thermoanalytical techniques, in particular thermogravimetric analysis (TGA) and derivative thermogravimetry (DTG), permit to find this information in a simple and straight forward method [1]. The non isothermal methods are the most commonly used for performing the kinetic analysis of solid state reactions. In order to fit the obtained data, a lot of kinetic methods have been proposed so as to obtain the parameters that characterize the thermal degradation process [2,3].

Non-isothermal kinetics can be classified into model-free, also called the isoconversional method, and model-fitting categories. In the first case, the reaction rate is supposed constant to the conversion extent (α) and only depends on the temperature (T) [4]. Isoconversional models are Kissinger [5], Flynn-Wall-Ozawa (FWO) and distributed activation energies model (DAEM) methods [6,7].

A model-fitting is the method used by Karaosmanoglu and Cift. (linear regression multiple) [8]. In this case, the Arrhenius equation is linearized to determine the kinetic parameters.

Coats–Redfern equation is also classified as a model fitting and it

* Corresponding author.
E-mail address: rrodri@unsj.edu.ar (R. Rodriguez).

https://doi.org/10.1016/j.jece.2017.12.013
Received 29 September 2017; Received in revised form 1 December 2017; Accepted 6 December 2017
Available online 09 December 2017
2213-3437/

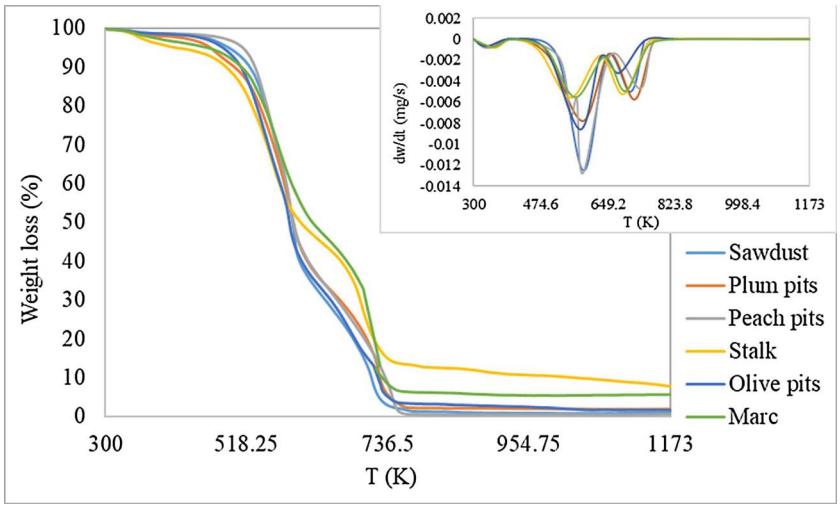

Fig. 1. TG and DTG curves for the studied biomass samples at 5K/min.

derives from the integral approach Arrhenius equation.

Garcia-Maraver et al. [9]. analyzed the decomposition under oxidative atmosphere of agricultural residues from olive trees at different heating rates using model-based and model-free methods. These authors determined the *E* values by the model-free methods, of which FWO and Kissinger-Akahira-Sunose (KAS) were the most appropriate, and they used the Coats-Redfern model-based method to determine the kinetic triplet. They deduced that the most feasible reaction order was one.

Jankovíc et al. [10] studied the decomposition under oxidative atmosphere of bones in the temperature range equal to 293–923 K. Friedman, FWO and KAS isoconversional methods were used to determine the *E* value. These researchers observed that the *E* value varies widely with the α value. Instead, these authors founded that the autocatalytic two parameter Sestak–Berggren (SB) model describe the combustion second stage, however, the third stage is described suitably by an n-th reaction order model.

Alvarez et al. [11] analyzed the combustion of most common biomass of Spain using TGA. They proposed a two-stage reaction model and they obtained the kinetic parameters from model-based methods. On the other hand, these researched observed that FWO and KAS model-free methods are not suitable to determine the kinetic parameters of biomass combustion.

Taking into account the different results obtained by several authors, the objective of this paper is to study the kinetics of the thermal decomposition of six wastes, sawdust, marc, stalk, plum, peach and olive pits by thermogravimetric analysis (TGA-DTA) at different heating rates (5, 10, 15 K/min) in oxidative atmosphere, applying different isoconversional and model-fitting methods in order to obtain the kinetic parameters. Further, the values of the changes of entropy (ΔS), enthalpy (ΔH) and free Gibbs energy (ΔG) for activated complex were calculated.

2. Materials and methods

2.1. Solid biomass wastes

Six regional wastes were used in this work: peach, plum and olive pits from canneries and jam-industries, marc and stalk from wineries, and sawdust from the timber industry. All these industries are located in the San Juan province, Argentine. The wastes were milled and sieved, the resulting 0.1-0.21 mm size fraction was used for the thermogravimetric tests. The selected particles size avoids mass transfer phenomenon limitations, it affects the reactions when the particle size is greater than 2 mm [12,13].

2.2. Proximate and ultimate analysis

The moisture, ash and organic matter content were determined according to ASTM standards (ASTM D1102-84 [14] and ASTM E872-82 [15]). Elemental analysis of the samples was performed using EuroEA3000 elemental analyzer. In order to calculate the high heating value, the correlation proposed by Sheng y Azevedo [16], was used:

$$HHV\,[MJ/Kg] = -1.3675 + 0.3137C + 0.7009H + 0.0318O \quad (1)$$

were *C* and *H* are the content of carbon and hydrogen (percentage on weight), respectively. *O* is the sum of the oxygen content and other elements included in the organic matter, i.e. *O = 100-C-H-Ash.*

2.3. Thermogravimetric and differential thermal analysis

A series of non-isothermal experiments were conducted for thermogravimetric analysis (TGA) and differential thermal analysis (DTA) using the Shimadzu analyzer (DTG-60). The used heating rate was equal to 5, 10 and 15 K/min; the temperature range was 302–1173 K. Approximately 12 mg of agro-industrial wastes samples were placed in the equipment. The experiments were carried out with dried samples. The data were recorded by a data logging system, which provided listings of sample weights and temperatures with time. To simulate the combustion, the composition of the used oxidative atmosphere was: 79% nitrogen and 21% oxygen with a flow rate equal to 100 mL/min, for each agro-industrial waste and heating rate. The Figs. 1–6 shows values of these experiments.

2.4. Thermodynamic parameters calculation

The thermodynamic properties; variations of enthalpy (ΔH), free Gibbs energy (ΔG), both in kJ/mol, and entropy (ΔS) in kJ/molK were calculated according the methodology proposed by Kim et al. [17]:

$$\Delta H = E - RT \quad (2)$$

$$\Delta G = E + RT_m Ln\left(\frac{k_b T_m}{hA}\right) \quad (3)$$

$$\Delta S = \frac{\Delta H - \Delta G}{T_m} \quad (4)$$

Where *E* is the activation energy (kJ/mol), *A* is the pre-exponential factor (s^{-1}), k_b is Boltzmann constant ($1.38\ 10^{-23}$ JK^{-1}), *h* is Plank constant (equal to $6.63\ 10^{-34}$ Js) and T_m is DTG peak temperature in K (temperature of the maximum mass loss rate). *E* and *A* for each sample were calculated with the kinetic method recommended in this study.

Table 1
Expressions for the most common reaction mechanisms in solid state reactions.

Reaction order	
Zero order	α
First order	$-\ln(1-\alpha)$
nth order	$(n-1)^{-1}(1-\alpha)^{1-n}$
Diffusional	
One dimensional diffusion	α^2
Two dimensional diffusion	$(1-\alpha)\ln(1-\alpha)+\alpha$
Three dimensional diffusion (Jander)	$[1-(1-\alpha)^{1/3}]^2$
Three dimensional diffusion (Ginstling – Brounstein)	$(1-2\alpha/3)-(1-\alpha)^{2/3}$
Nucleation	
Power law	α^n; n = 3/2, 1, ½, 1/3, 1/4
Exponential law	α
Avrami − Erofeev	$[-\ln(1-\alpha)](1/n)$; n = 1, 2, 3, 4
Contracting geometry	
Contracting area	$(1-\alpha)^{(1/n)}$; n = 2
Contracting volume	$(1-\alpha)^{(1/n)}$; n = 3

2.5. Kinetic analysis

There are two main mathematical approaches to obtain the kinetics data from the thermogravimetric data: model-free (isoconversional) methods and model-based (non-isoconversional) methods [18]. Model-free methods enable determination of kinetic parameters without knowledge of the reaction mechanism [19], while model-based methods permit the determination of the controlling reaction mechanism and reaction order.

2.5.1. Isoconversional method

2.5.1.1. Kissinger method. Kissinger's method assumes that the reaction rate has maximum value at the peak temperature (*Tm*). This assumption also implies a constant extent of conversion (α) at *Tm*. The Kissinger's equation [5] can be writing the following form:

$$d^2\alpha/dt^2]_{\alpha=\alpha_m} = E\beta/RT_m^2 + Aexp(E/RT_m)f'(\alpha_m) = 0 \quad (5)$$

Where, β *and* R are the heating rate (K/min) and the universal gas constant (0.008314 kJ/molK), respectively. Taking account that the reaction can be considering of first order, f(α) = (1 − α) so, f'(α) = 1.

Reordering and applying logarithms, Eq. (5) can be rewriting the following form:

$$ln(\beta/T_m^2) = -E/RT_m + ln[AR/E] \quad (6)$$

This method can be used independently of the conversion, therefore not need to know the reaction mechanism. By a plot of $ln(\beta/T_m^2)$ versus $1/T$ gives E and A from the slope and intersection point, respectively.

2.5.1.2. Flynn-Wall-Ozawa method (FWO). This method [7,20] was developed for non-isothermal analysis and used the Doyle's approximation [21] for determine the activation energy without knowing the reaction order. Finally, the equation represents this method is as follows:

$$ln\beta = ln(AE/Rg(\alpha)) - 5.331 - 1.052E/RT \quad (7)$$

where $g(\alpha)$ is the integral reaction model and is constant at a given value of conversion: $g(\alpha) = n^{-1}(-1 + (1-\alpha)^{-n})$ for reaction-order models. For a constant conversion, a plot of $ln\beta$ versus $1/T$, from the data at the different heating rates, leads to a straight line where the slope is equal to (E/R) and the frequency factor was calculated considering $n = 1$.

2.5.1.3. Distributed activation energy model method (DAEM). The distributed activation energy model (DAEM), originally developed by Vand [22], has been extensively used for analyzing the complex reactions occurring during the pyrolysis of fossil fuels. This model assumes that number of parallel irreversible first order reactions that have different kinetic parameters occur simultaneously. Base on reference (Bhavanam et al. [23]) E, A and $f(E)$ can be calculated by following equation:

$$ln\beta/T^2 = lnRA/E + 0.6075 - E/RT \quad (8)$$

Eq. (5) develops a linear relationship between $ln\beta/T^2$ and $1/T$ with the slope of $(-E/R)$. The E and A can be determined from the slope and intercept of the plots.

2.5.2. Non-isoconversional method

These methods are based on Arrhenius equation, which described the temperature dependence of the rate constant k for the process.

$$k(T) = Aexp\left(-\frac{E}{RT}\right) \quad (9)$$

2.5.2.1. Coats-Redfern method. Coats-Redfern method [24] is a model-based method that derives from the integral approach Arrhenius equation (Eq. (9)), the integration function is shown as below:

$$g(\alpha) = \int_0^\alpha \frac{d(\alpha)}{f(\alpha)} = \frac{A}{\beta}\int_0^T e^{-\frac{E}{RT}}dT \quad (10)$$

The Eq. (10) is integrated by Coats-Redfern method to be and the following expression is obtained:

$$ln\frac{g(\alpha)}{T^2} = ln\frac{AR}{E\beta} - \frac{E}{RT} \quad (11)$$

Plotting $g(\alpha)/T^2$ versus T and by nonlinear regression could be obtained activation energy E and pre-exponential factor A. There are different theoretical expressions of $g(\alpha)$, they are showed in Table 1.

2.5.2.2. Linear multiple regression method. Parameters of the reaction kinetics were determined using the procedure applied by Karaosmanoglu and Cift [8]. Global kinetics of the reaction can be written as:

$$\frac{-1}{w_0 - w_f}\frac{dw}{dt} = \left(\frac{w - w_f}{w_0 - w_f}\right)^n \quad (12)$$

where w_o is the initial mass at the start of that stage, w_f the final mass at the end of that stage, w the mass at any time, dw/dt the ratio of change in mass to change in time and n the order of the reaction. Applying the Arrhenius (Eq. (9)), the combined Eqs. (9) and (12) lead to a linear form Eq. (13) as:

$$Ln\left[\frac{-1}{w_0 - w_f}\frac{dw}{dt}\right] = Ln(A) - \left(\frac{E}{RT}\right) + nLn\left(\frac{w - w_f}{w_0 - w_f}\right) \quad (13)$$

This Eq. may be written under the linear form:

$$y = B + Cx + Dz \quad (14)$$

Where

$$y = Ln\left[\frac{-1}{w_0 - w_f}\frac{dw}{dt}\right] \quad (15)$$

$$x = \frac{1}{T} \quad (16)$$

$$z = Ln\left(\frac{w - w_f}{w_0 - w_f}\right) \quad (17)$$

$$B = Ln(A);\ C = -\frac{E}{R};\ D = n \quad (18)$$

Constants B, C, D were estimated by multi-linear regression of the TGA data for each stage using Microsoft Excel.

Table 2
Results of proximate and ultimate analysis (dry basis, weight percentage). High heating values (HHV).

	Peach pits	Stalk	Marc	Plum pits	Olive pits	Sawdust
C (%)	53.01	46.14	52.91	48.95	52.79	44.71
H (%)	5.90	5.74	5.93	1.38	2.57	1.48
N (%)	2.32	6.37	5.41	0.99	1.39	4.20
S (%)	1.88	4.21	5.34	0.27	0.50	0.28
O (%)*	36.89	37.54	30.41	48.41	42.75	49.33
Ash (%, dry basis)	1.30	10.16	8.81	0.73	2.33	1.19
Volatile Matter (%, total weight)	79.10	55.84	68.60	77.86	77.25	80.90
Fixed carbon (%, dry basis)	13.90	23.07	21.98	15.55	15.87	11.06
Moisture (%, total weight)	5.70	7.70	8.38	5.86	4.55	6.85
HHV (MJ/kg)	21.39	12.03	13.31	13.71	17.02	12.19

* By difference.

3. Results and discussion

3.1. Biomass characterization

Table 2 shows the results obtained by ultimate and proximate analysis for the six wastes. Taking into account the first analysis, the marc has the highest carbon (52.91%) and hydrogen (5.93%) contents. Furthermore, the stalk has the highest nitrogen content (6.37%). among the six materials. The results are in agreement with those of other investigators [25–27].

The immediate analysis results show the moisture content of all analyzed biomass wastes varies between 4.55 and 8.38%. It is necessary to consider that a high-water content increases the energy requirements to carry out the thermal treatment, rises the residence time for drying and reduces the temperature, resulting in incomplete conversion of the hydrocarbons. These aspects decrease the process efficiency.

Regarding the ash content of the agro-industrial wastes, it presents a great variation, between 0.73 and 10.16% for plum pits and stalk, respectively. It is significant to note that the presence of alkali metals and chlorine causes the components of the ash melt and volatilize at low temperatures, even though, their total concentration in biomass is usually lower than that of coal. Fortunately, the six agro-industrial wastes have a low percentage of ash, affecting positively the high heating value (HHV) [16]. The high content of organic matter makes these wastes very suitable for thermal treatment [28].

3.2. Thermogravimetric analysis

The obtained TG and DTG curves for all studies wastes at different heating rate can be observed in Figs. 1–6. During the combustion process, different stages can be observed: first, drying and light volatile release (T < 393 K); second, devolatilization (393 K < T < 723 K); third, char combustion (723 K < T < 873 K) and the last, residual combustion (T > 873 K). These stages are associated with the peaks in the DTG curves and thus with the changes of the slopes of the TG curves. Most weight loss occurs in the devolatilization stage, giving average values equal to 56, 55, 54, 42, 45 and 43% for peach, olive and plum pits, stalk, marc and sawdust, respectively (average values). These differences are due to the different wastes compositions. Comparing the weight loss rate for the studied wastes during this stage, the sawdust showed the highest value of this parameter at all heating rates and the marc, the lowest value. The temperature for the maximum decomposition rate in this stage depends on the agro-industrial waste composition.

Another step in which occurs a high weight loss is the char combustion: 25, 29, 27, 31, 38, and 23% for peach, olive and plum pits, stalk, marc and sawdust, respectively (average values) These differences are due to the different wastes compositions. When the temperature increases during the heat-up, the evolution of different products or groups of products occurs in segmented (but overlapping) phases. During the first stage, the moisture evolution is produced, then the gases release occurs. According other authors, primarily CO_2 and CH_4 are generated, and later it is connected with the release of chemically bonded CO_2 and chemically formed H_2O. At temperature higher than 873 K, species such as carbon oxides, tars, and hydrocarbon gases (heavy hydrocarbons such as fluorene, phenanthrene, fluoranthene, and benzo (a) pyrene) were identified in the gas phase. At higher temperatures, carbon oxides are the primary products [29].

Other authors [9–11] have found the same three stages for biomass combustion process too and the range for each they are similar to this work.

3.3. Differential thermal analysis

The results of the differential thermal analyses are show in Figs. 4–6. The maximum peaks on the DTA curves show the level of exothermic reactions, whereas the minimum show the level of endothermic reactions during the thermal decomposition of the studied wastes. The small endotherms on the DTA curves observed at the temperature of 350 K were due to the evaporation of water from the samples. The two exothermic peaks represented the two successive reactions taking place during the thermal decomposition under oxidative atmosphere of the biomass samples.

The first exothermic reactions started at temperatures over 473 K and reached their peak values at the temperatures of 600, 615 and 630 K (approximately for all wastes) for the heating rates of 5, 10 and 15 K/min, respectively. The second exothermic reactions started at 670 K and their peaks occurs at 700, 740 and 760 K for the same heating rates. These curves show that the temperature difference due to these exothermic reactions were in the range of 200–860 μV for all cases.

3.4. Thermodynamic properties

Table 3 shows the results obtained of the thermodynamic parameters of activated complex formation, ΔH, ΔG and ΔS, were calculated at the temperature of the maximum weight loss rate is produced [17].

The Gibbs free energy, also known as free enthalpy, is a function extensive and expresses the equilibrium condition and spontaneity of a chemistry reaction (at constant pressure and temperature). The obtained ΔG values are positives in all cases, showing the total system energy growth at the reagents approach and the activated complex formation. It is a widespread analysis of the heat flow and disorder change. A higher ΔG value shows a lower reaction favorability.

On the other hand, enthalpy is a measurement of energy in a thermodynamic system. Enthalpy is defined as a state function and it depends only on the prevailing equilibrium state identified by the internal energy, pressure, and volume. It is an extensive quantity. ΔH is equal to difference between the reagent and the activated complex, agreeing with the activation energies. The ΔH values positive presented that an external energy source is necessary to increase the reagents energy level to their transition state, showing that the combustion reaction were all endothermic. Moreover, higher enthalpy values mark a less reactive system [30,31].

All obtained ΔS values associated with the formation of complex activated species are negative showing the combustion process was developed from disordered-state to ordered-state. When $\Delta S < 0$, the material has just passed through some kind of physical or chemical aging process, bringing it to a state near its own thermodynamic equilibrium. In this situation, the material shows little reactivity [32].

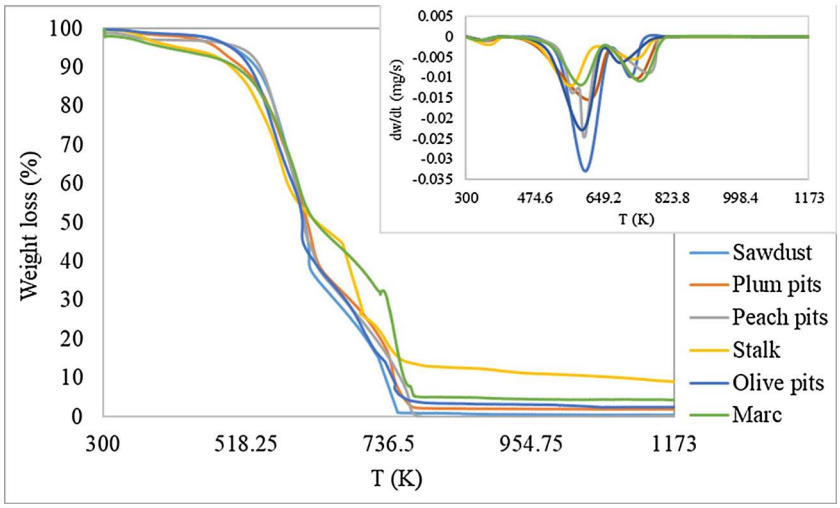

Fig. 2. TG and DTG curves for the studied biomass samples at 10K/min.

3.5. Kinetic analysis

3.5.1. Kissinger method

Figs. 7 and 8 shows the lines obtained from Eq. (6). Using these methods, the activation energy was obtained at the temperature of maximum reaction rate. This temperature, for all cases, has been determined from the first derivative of the curves at different heating rate.

The obtained values for this parameter vary between 52.75-116.92 kJ/mol and 65.39–157.24 kJ/mol for devolatilization and char combustion stages, respectively (Table 4). The activation energy was highest for plum pits in the third stage and for olive pits in the second stage, in the two cases the smallest value was to marc. Due to the E is the necessary minimum energy for the reaction occurrence and, according to the found E values, the marc presents the best combustion performance.

Pre-exponential factor were calculated from Eq. (6) derived from the intercept of plotting regression line. The results obtained vary between 1.21 10^{04} to 7.96 $10^{09}\,s^{-1}$ and 1.36 10^{04} to 9.94 $10^{10}\,s^{-1}$ for devolatilization and char combustion stages, respectively. This parameter represents the fraction of molecules that would react if either the energy activation was zero.

3.5.2. Flynn-Wall-Ozawa method (FWO)

For the investigated process, activation energy was evaluated from the straight line slope of Eq. (7). Fig. 9 presents the variation of *E* with α for all wastes studied. Different behaviors are observed for solid wastes, however for conversion between 0.2 and 0.6 the *E* was the similar tendency. Due to the activation energy is dependent on conversion for all cases, the reaction mechanism is not the same in the whole decomposition process indicating the existence of a complex multi-step mechanism that occurs in the solid state [33].

The obtained average values of this parameter vary between 136.71 and 261.10 kJ/mol for all studied agro-industrial (Table 5). The pre-exponential factor varies between 9.41 10^{04} and 3.72 $10^{22}\,s^{-1}$

3.5.3. Distributed activation energy model method (DAEM)

The kinetic analysis included recording of weight loss curves at different heating rate in order to deduce the dependence of kinetic parameters on conversion level. The Eq. (8) was used to calculate the values of activation energy at each selected level of conversion rate α from the Arrhenius plot of $ln\ (\beta/T^2)$ versus $1/T$. The conversions from 0.1 to 0.7 was used, it is due to the fact that for higher conversions the plots are nonlinear and show different behavior due to the different chemical reactions occur [27]. This behavior suggests that the materials have different kinds of reaction mechanisms at the end of the decomposition process (residual combustion), for that the conversions between 0.1 and 0.7 was considered for describing the application of DAEM. The activation energy values are reported in Table 5. The *E* dependence with α shows that the decomposition is not a single reaction stage, but includes the contributions of parallel reaction steps on the global reaction rate (Fig. 10). In this way, global kinetic parameters are less useful for studying the thermal degradation of the fuels since

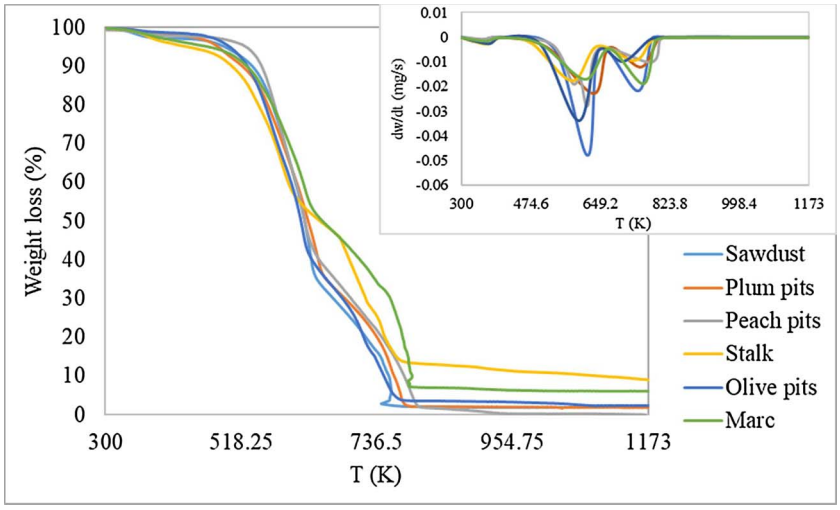

Fig. 3. TG and DTG curves for the studied biomass samples at 15K/min.

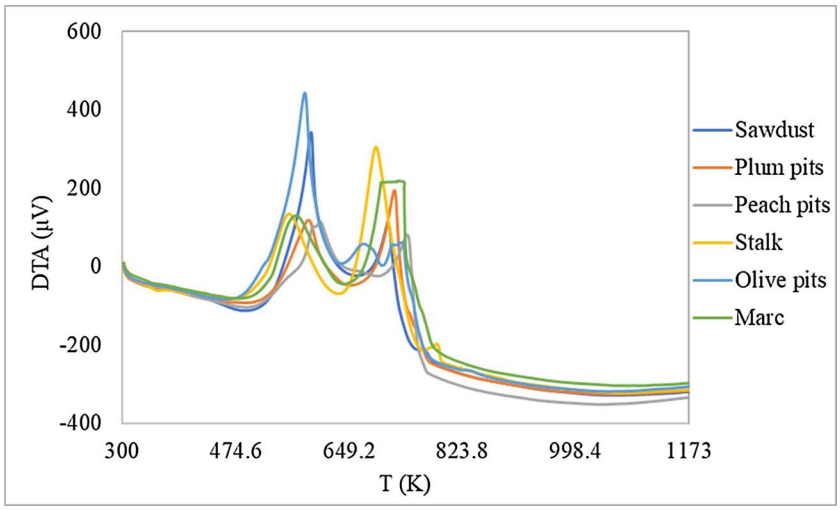

Fig. 4. DTA curves for the studied biomass samples at 5K/min.

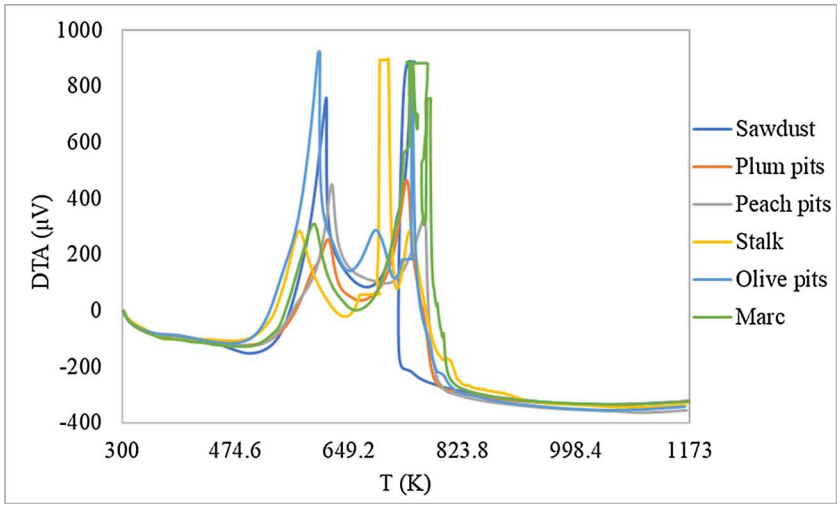

Fig. 5. DTA curves for the studied biomass samples at 10K/min.

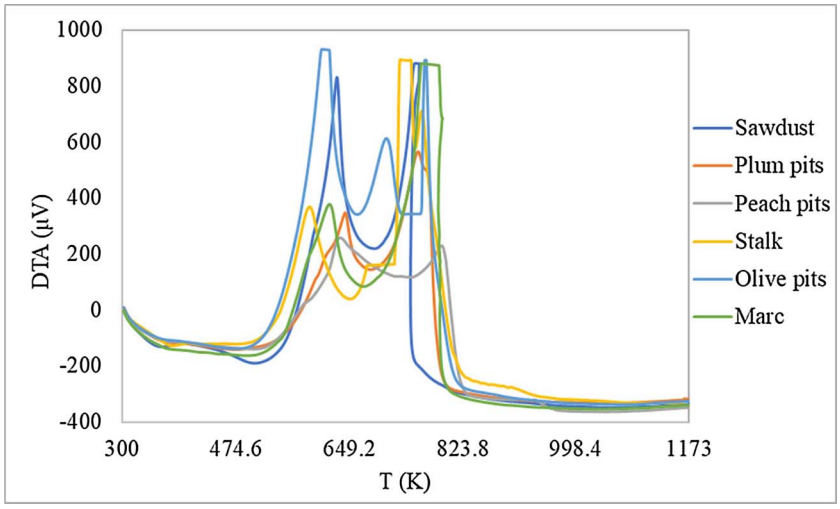

Fig. 6. DTA curves for the studied biomass samples at 15K/min.

particular reactions not can be defined [34]. Nevertheless, this analysis is relevant in order to obtain general tendencies, with particular regard to the assessment of the reactivity of the fuels.

3.5.4. Coats-Redfern method

Tables 6 and 7 show the obtained kinetics parameters and the statistical parameter values for different studied agro-industrial wastes. The best fitting is presented for the contraction volume and first order models for devolatilization and char combustion stages, respectively. These models describe the combustion characteristics of biomass wastes obtained by non-isothermal TGA and it assumes that nucleation occurs rapidly on the surface of the particle. The rate of degradation is

Table 3
Variations of enthalpy, free Gibbs energy and entropy obtained for all biomass.

Biomass	Atmosphere	β (K/min)	Thermodynamic parameters		
			ΔH (kJ/mol)	ΔG (kJ/mol)	ΔS (KJ/mol K)
Sawdust	Devolatilization	5	79.96	156.09	−0.13
		10	109.36	100.31	0.02
		15	104.24	101.08	0.01
	Char combustion	5	87.56	189.84	−0.14
		10	82.38	190.52	−0.15
		15	68.75	150.56	−0.11
Plum pits	Devolatilization	5	79.95	99.90	−0.03
		10	98.18	101.13	0.00
		15	92.96	101.69	−0.01
	Char combustion	5	140.03	191.50	−0.07
		10	180.80	192.05	−0.02
		15	189.14	194.92	−0.01
Peach pits	Devolatilization	5	76.31	99.86	−0.04
		10	94.82	97.20	0.00
		15	101.99	97.47	0.01
	Char combustion	5	186.21	192.70	−0.01
		10	168.49	195.80	−0.04
		15	137.39	194.64	−0.07
Olive pits	Devolatilization	5	69.93	99.52	−0.05
		10	91.54	100.20	−0.01
		15	98.51	97.55	0.00
	Char combustion	5	101.27	185.86	−0.12
		10	164.68	188.38	−0.03
		15	168.13	187.92	−0.03
Stalk	Devolatilization	5	60.30	97.88	−0.07
		10	67.16	98.86	−0.06
		15	75.87	99.87	−0.04
	Char combustion	5	100.45	187.25	−0.13
		10	97.39	189.53	−0.13
		15	155.14	188.84	−0.05
Marc	Devolatilization	5	73.09	98.99	−0.05
		10	93.01	100.32	−0.01
		15	97.66	101.28	−0.01
	Char combustion	5	142.52	190.76	−0.07
		10	181.35	193.32	−0.02
		15	112.50	200.74	−0.12

controlled by the resulting reaction interface progress toward the center of the solid [35].

For this model, the R^2 value was between 0.97–0.99. Fig. 11 show the comparison of experimental data and the predicted values for marc and plum pits, respectively, at different heating rates.

The activation energy's values calculated vary slightly with the heating rate due to heat effect increase [36,37]. When the heating rate increases, higher temperature is required in order to set off the combustion process.

The calculated values of pre-exponential factor were between 8.68 10^9 and 2.08 10^{14} s^{-1} and between 5.82 10^5 and 1.45 10^{13} s^{-1} for the devolatilization and char combustion stage, respectively. This parameter also augments with the heating rate increase.

3.5.5. Linear multiple regression method

Fig. 12 shows the comparison between the experimental data and the model results. The founded activation energies and pre-exponential factors and reaction orders of the devolatilization and char combustion steps were shown in Tables 7 and 8, respectively. Since activation energy is minimum energy requirement to start a reaction, higher values of this parameter mean slower reactions and can also be used for determination of reactivity of a fuel. For all cases, the reaction order n is smaller to 1.

The obtained R^2 values (Tables 6 and 7) is an indicator of the fitted model to experimental data and they vary between 0.83 and 0.95.

3.5.6. Comparison between different analyzed methods

The obtained results from the single heating rate kinetic methods (linear multiple regression and Coats-Redfern) and multiple heating rate kinetic methods (Kissinger, Flynn-Wall-Ozawa and DAEM) are very different. These differences are explained by the equation parameters and assumptions taking into account by each method.

However, Garcia-Maraver et al. [9] obtained similar E values using FWO, KAS and Coats-Redfern kinetic methods for the decomposition under oxidative atmosphere of agricultural residues from olive trees.

The activation energy values obtained using Kissinger method (Table 4) are consistent with the values range obtained by the FWO and DAEM methods and are very near to their average values. On the other hand, using the Coats-Redfern and regression linear methods, the obtained energy activation values are very different. Table 8 shows the average values comparison between all methods used.

The FWO and DAEM methods allow estimating activation energy and pre-exponential factor values as a function of conversion with a good agreement. However, Kissinger method give a single *E* value for the whole process and the process complexity may not be exposed. On the other hand, the linear multiple regression and Coats–Redfern methods produce different *E* values for each considered heating rates, showing that the kinetic rate is controlled by the occurrence of different phenomena which is not mass dependent.

Considering that other authors applied Coast Redfern method to biomass combustion [9] [11], it is observed that they obtained different kinetic model for both studied stage to the proposed model in this work.

On the other hand, the obtained kinetic parameters in literature, applying several kinetic methods, are different to those reported for

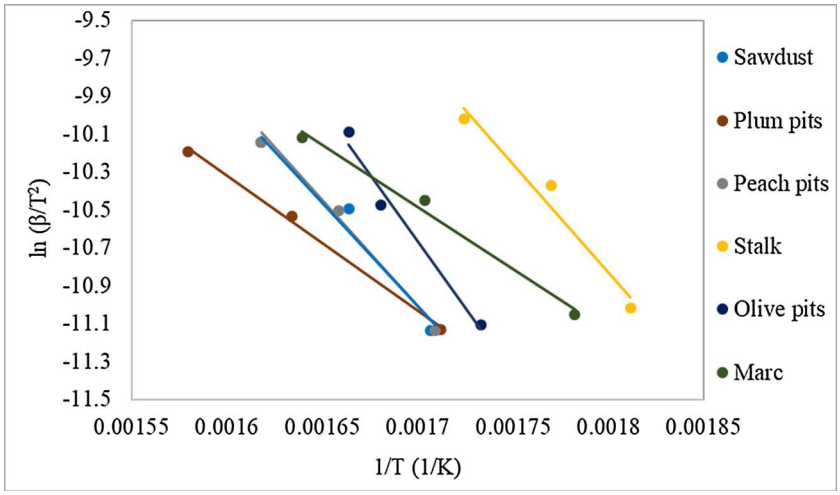

Fig. 7. Kissinger method applied to all biomass at different heating rates for devolatilization stage.

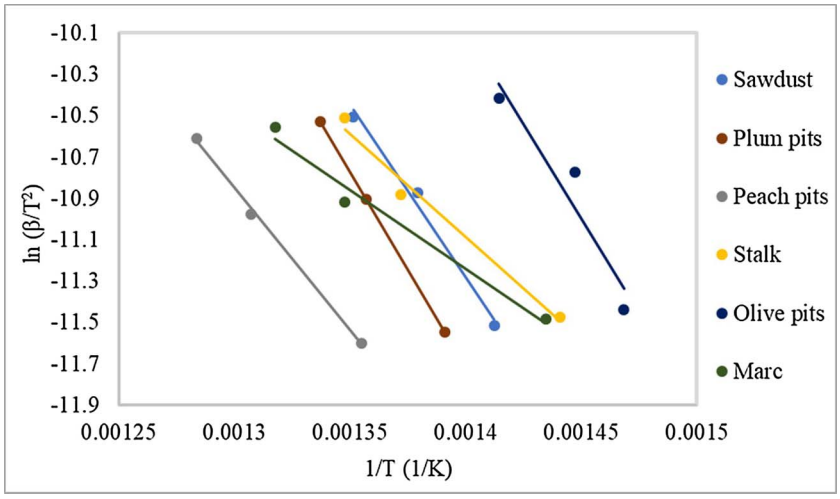

Fig. 8. Kissinger method applied to all biomass at different heating rates for char combustion stage.

Table 4
Pre-exponential factor and activation energy obtained using Kissinger method.

Wastes	Sawdust	Plum pits	Peach pits	Olive pits	Stalk	Marc
Parameters						
Devolatilization stage						
E (kJ/mol)	92.99	59.14	90.64	116.92	94.53	52.75
A (s^{-1})	3.35 10^{07}	2.05 10^{04}	2.02 10^{07}	7.96 10^{09}	1.75 10^{08}	1.21 10^{04}
R^2	0.98	1	0.99	0.98	0.98	0.97
Char combustion stage						
E (kJ/mol)	138.26	157.24	114.38	151.98	82.82	65.39
A (s^{-1})	2.71 10^{09}	4.85 10^{10}	1.55 10^{07}	9.94 10^{10}	1.73 10^{05}	1.36 10^{04}
R^2	0.96	0.99	0.99	0.97	0.96	0.98

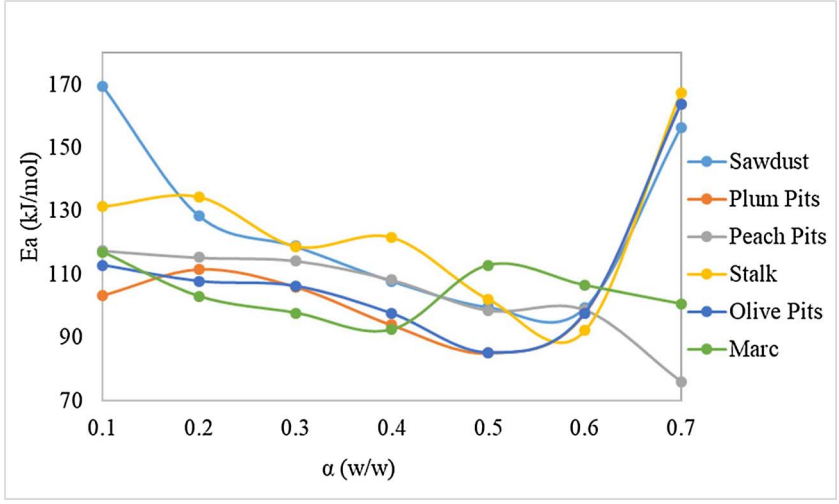

Fig. 9. Dependence of activation energy on the extent of conversion evaluated from the FWO method.

other authors [9–11]. It can be due to the complexity of the wastes composition.

4. Conclusions

- The TG curves analysis showed that their combustion decomposition is divided into four stages according to the weight loss rate: the water and light volatile release, devolatilization, char and residual combustions.
- The DTA curves showed small endotherms at the temperature of 350 K were due to the evaporation of water, then two exothermic peaks represented the two successive reactions taking place during the thermal decomposition under oxidative atmosphere.
- Different kinetic methods were applied to the obtained non-isothermal data. The obtained activation energy values applying these methods are very dissimilar.
- DAEM and FWO methods can reflect the *E* and *A* distribution of the whole combustion process. But, due to the of existing the very large variation of *E* on α, the kinetic model determination can be unreliable, since in that case the calculated values of *E*, do not represent the real values.
- By Coats-Redfern method, the reaction mechanisms for each stage were obtained. The models of volume contraction and first order describe the devolatilization and char combustion stages,

Table 5
Activation energy for conversion range of 0.1–0.7 using FWO and DAEM methods.

Agro-industrial wastes	α	DAEM model			FWO model			Difference (%)
		E (kJ/mol)	A (s^{-1})	R^2	E (kJ/mol)	A (s^{-1})	R^2	
Sawdust	0.1	169.37	$1.71\ 10^{16}$	0.99	169.34	$3.72\ 10^{22}$	0.99	0.02
	0.2	128.48	$2.52\ 10^{11}$	0.99	130.95	$6.18\ 10^{17}$	0.99	1.89
	0.3	118.89	$1.27\ 10^{10}$	0.99	122.10	$3.36\ 10^{16}$	0.99	2.63
	0.4	107.86	6.10^{08}	0.99	111.86	$1.71\ 10^{15}$	0.99	3.58
	0.5	99.68	$6.59\ 10^{07}$	0.99	104.29	$1.95\ 10^{14}$	0.99	4.42
	0.6	99.39	$4.74\ 10^{07}$	0.99	104.18	$1.37\ 10^{14}$	0.99	4.60
	0.7	156.47	$8.61\ 10^{11}$	0.98	158.96	$2.81\ 10^{18}$	0.98	1.57
	Average	125.73	$2.45\ 10^{15}$		128.81	$5.31\ 10^{21}$		
Plum pits	0.1	103.39	$9.68\ 10^{09}$	0.99	106.31	$3.45\ 10^{06}$	0.99	2.75
	0.2	111.61	$8.94\ 10^{09}$	0.99	114.77	$3.48\ 10^{06}$	0.99	2.75
	0.3	106.05	$9.30\ 10^{08}$	0.99	109.82	$1.27\ 10^{06}$	0.99	3.43
	0.4	94.00	$3.58\ 10^{07}$	0.99	111.86	$3.17\ 10^{05}$	0.99	15.97
	0.5	85.19	$2.89\ 10^{06}$	0.99	90.56	$9.41\ 10^{04}$	0.99	5.93
	0.6	97.65	$2.20\ 10^{07}$	0.98	102.68	$2.43\ 10^{05}$	0.97	4.90
	0.7	163.91	$1.48\ 10^{12}$	0.99	166.32	$3.93\ 10^{07}$	0.96	1.45
	Average	103.39	$9.68\ 10^{09}$		114.62	$6.88\ 10^{06}$		
Peach pits	0.1	117.50	$5.41\ 10^{10}$	0.99	120.25	$1.26\ 10^{17}$	0.99	2.29
	0.2	115.31	$1.22\ 10^{10}$	0.99	118.46	$3.06\ 10^{16}$	0.99	2.66
	0.3	114.28	$4.68\ 10^{09}$	0.99	117.74	$1.24\ 10^{14}$	0.99	2.94
	0.4	108.21	$6.34\ 10^{08}$	0.99	112.24	$1.79\ 10^{15}$	0.99	3.59
	0.5	98.59	$5.25\ 10^{07}$	0.99	103.28	$1.56\ 10^{14}$	0.99	4.54
	0.6	98.76	$2.58\ 10^{07}$	0.98	103.82	$8.33\ 10^{13}$	0.98	4.87
	0.7	76.10	$8.47\ 10^{04}$	0.80	83.04	$3.29\ 10^{11}$	0.75	8.36
	Average	104.11	$1.16\ 10^{10}$		108.40	$2.27\ 10^{16}$		
Olive pits	0.1	112.89	$5.49\ 10^{10}$	0.99	115.49	$1.17\ 10^{17}$	0.99	2.25
	0.2	107.79	$4.49\ 10^{09}$	0.99	111.05	$1.06\ 10^{16}$	0.99	2.94
	0.3	106.26	$1.37\ 10^{09}$	0.99	109.89	$3.49\ 10^{15}$	0.99	3.30
	0.4	97.55	$8.93\ 10^{07}$	0.99	101.90	$2.45\ 10^{14}$	0.99	4.27
	0.5	85.19	$2.88\ 10^{06}$	0.99	90.56	$8.75\ 10^{12}$	0.95	5.93
	0.6	97.64	$2.20\ 10^{07}$	0.98	102.68	$7.01\ 10^{13}$	0.70	4.91
	0.7	163.91	$1.48\ 10^{12}$	0.99	166.32	$5.17\ 10^{18}$	0.75	1.45
	Average	110.18	$2.32\ 10^{11}$		113.98	$4.15\ 10^{17}$		
Stalk	0.1	131.38	$3.49\ 10^{13}$	0.98	132.62	$6.55\ 10^{19}$	0.98	0.94
	0.2	134.36	$4.52\ 10^{12}$	0.99	136.11	$1.00\ 10^{19}$	0.99	1.29
	0.3	118.83	$3.30\ 10^{10}$	0.99	121.73	$8.11\ 10^{16}$	0.99	2.38
	0.4	121.64	$2.48\ 10^{10}$	0.99	124.71	$6.54\ 10^{16}$	0.99	2.46
	0.5	102.2	$2.83\ 10^{10}$	0.99	106.62	$3.85\ 10^{14}$	0.99	4.15
	0.6	92.19	$2.78\ 10^{06}$	0.99	97.96	$9.80\ 10^{12}$	0.99	5.89
	0.7	167.35	$8.62\ 10^{11}$	0.98	170.05	$3.27\ 10^{18}$	0.92	1.59
	Average	123.99	$5.77\ 10^{12}$		127.11	$1.11\ 10^{19}$		
Marc	0.1	117.03	$2.17\ 10^{11}$	0.88	119.39	$4.56\ 10^{17}$	0.90	1.98
	0.2	103.01	$1.14\ 10^{09}$	0.99	106.69	$2.81\ 10^{15}$	0.99	3.45
	0.3	97.78	$1.29\ 10^{08}$	0.99	102.07	$3.48\ 10^{14}$	0.99	4.20
	0.4	92.49	$1.95\ 10^{07}$	0.99	97.37	$5.69\ 10^{13}$	0.99	5.01
	0.5	112.91	$5.96\ 10^{08}$	0.98	117.16	$1.85\ 10^{15}$	0.96	3.63
	0.6	106.54	$2.81\ 10^{07}$	0.99	111.92	$1.04\ 10^{14}$	0.93	4.81
	0.7	100.65	$2.62\ 10^{06}$	0.99	106.98	$1.11\ 10^{13}$	0.72	5.92
	Average	104.34	$3.13\ 10^{10}$		108.80	$3.75\ 10^{14}$		

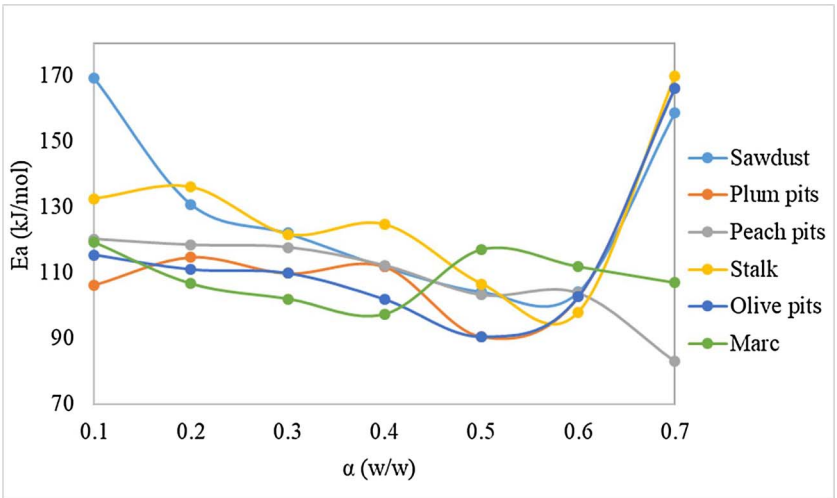

Fig. 10. Dependence of activation energy on the extent of conversion evaluated from the DAEM method.

Table 6
Pre-exponential factor and activation energy obtained by Coats-Redfern and linear multiple regression methods in the devolatilization stage.

Agro-industrial wastes	Coats-Redfern				Linear multiple regression				
	β (K/min)	E (KJ/mol)	A (s^{-1})	R^2	E (KJ/mol)	A (s^{-1})	n	R^2	Difference (%)
Sawdust	5	84.83	$5.63\ 10^{11}$	0.98	91.37	$5.81\ 10^{05}$	0.72	0.92	7.16
	10	114.36	$2.08\ 10^{14}$	0.98	92.14	$8.41\ 10^{05}$	0.60	0.92	19.43
	15	109.38	$6.47\ 10^{13}$	0.98	89.72	$5.33\ 10^{05}$	0.65	0.92	17.97
Plum pits	5	84.81	$5.43\ 10^{11}$	0.99	77.28	$2.51\ 10^{04}$	1.02	0.91	9.74
	10	103.27	$1.94\ 10^{13}$	0.98	58.21	$4.24\ 10^{02}$	0.64	0.92	43.63
	15	98.22	$6.82\ 10^{12}$	0.99	55.12	$2.52\ 10^{02}$	0.52	0.94	43.88
Peach pits	5	81.17	$2.61\ 10^{11}$	0.99	87.23	$2.31\ 10^{05}$	0.76	0.83	6.95
	10	99.83	$2.12\ 10^{13}$	0.99	87.43	$2.83\ 10^{05}$	0.82	0.86	12.42
	15	107.13	$8.43\ 10^{13}$	0.99	82.52	$1.03\ 10^{05}$	0.77	0.87	22.97
Stalk	5	64.89	$8.68\ 10^{9}$	0.98	60.58	$9.97\ 10^{03}$	0.86	0.88	6.64
	10	71.86	$3.75\ 10^{10}$	0.98	60.48	$1.67\ 10^{03}$	0.68	0.91	15.84
	15	80.69	$2.26\ 10^{11}$	0.99	61.07	$2.38\ 10^{03}$	0.76	0.91	24.32
Olive pits	5	74.73	$6.80\ 10^{10}$	0.99	64.73	$2.05\ 10^{03}$	0.79	0.88	13.38
	10	96.51	$5.92\ 10^{12}$	0.98	64.90	$3.31\ 10^{03}$	0.55	0.88	32.75
	15	103.50	$4.12\ 10^{13}$	0.98	69.10	$1.01\ 10^{04}$	0.78	0.92	33.24
Marc	5	77.75	$1.23\ 10^{11}$	0.99	64.35	$1.42\ 10^{03}$	0.93	0.83	17.23
	10	97.89	$7.43\ 10^{12}$	0.99	60.77	$9.62\ 10^{02}$	0.70	0.85	37.92
	15	102.73	$1.69\ 10^{13}$	0.98	55.37	$3.33\ 10^{02}$	0.57	0.91	46.10

Table 7
Pre-exponential factor and activation energy obtained by Coats-Redfern and linear multiple regression methods in the char combustion stage.

Agro-industrial wastes	Coats-Redfern				Linear multiple regression				
	β (K/min)	E (KJ/mol)	A (s^{-1})	R^2	E (KJ/mol)	A (s^{-1})	n	R^2	Difference (%)
Sawdust	5	93.45	$1.14\ 10^{6}$	0.98	125.99	$6.13\ 10^{06}$	0.84	0.84	25.83
	10	88.37	$5.82\ 10^{5}$	0.98	70.79	$4.37\ 10^{02}$	0.72	0.86	19.89
	15	74.94	$7.60\ 10^{7}$	0.99	134.80	$2.75\ 10^{07}$	0.70	0.89	44.41
Plum pits	5	146.01	$7.41\ 10^{9}$	0.99	132.15	$1.21\ 10^{07}$	0.95	0.80	9.49
	10	186.93	$6.65\ 10^{12}$	0.99	93.56	$1.70\ 10^{04}$	0.72	0.89	49.95
	15	195.36	$1.67\ 10^{13}$	0.99	121.10	$1.74\ 10^{06}$	0.79	0.96	38.01
Peach pits	5	192.35	$1.45\ 10^{13}$	0.99	116.34	$5.42\ 10^{05}$	0.71	0.85	39.52
	10	174.85	$5.91\ 10^{11}$	0.96	138.12	$2.01\ 10^{07}$	0.73	0.95	21.01
	15	143.87	$6.39\ 10^{9}$	0.98	136.79	$1.24\ 10^{07}$	0.78	0.94	4.92
Stalk	5	106.22	$1.15\ 10^{7}$	0.99	91.38	$1.37\ 10^{04}$	0.85	0.83	13.97
	10	103.45	$1.03\ 10^{7}$	0.98	111.81	$4.41\ 10^{05}$	0.59	0.83	7.48
	15	161.31	$1.78\ 10^{11}$	0.98	73.30	$6.79\ 10^{03}$	0.69	0.94	54.56
Olive pits	5	106.93	$1.25\ 10^{7}$	0.98	36.07	$5.69\ 10^{03}$	0.51	0.84	66.27
	10	170.42	$6.31\ 10^{11}$	0.98	23.69	$1.06\ 10^{03}$	0.47	0.86	86.10
	15	174.01	$1.38\ 10^{12}$	0.98	46.31	$8.48\ 10^{02}$	0.64	0.92	73.39
Marc	5	148.31	$9.55\ 10^{9}$	0.99	55.09	1.10^{02}	0.47	0.76	62.85
	10	187.38	$5.63\ 10^{12}$	0.97	53.83	$1.80\ 10^{02}$	0.22	0.84	71.27
	15	118.81	$3.63\ 10^{7}$	0.99	97.47	$2.55\ 10^{04}$	0.66	0.92	17.96

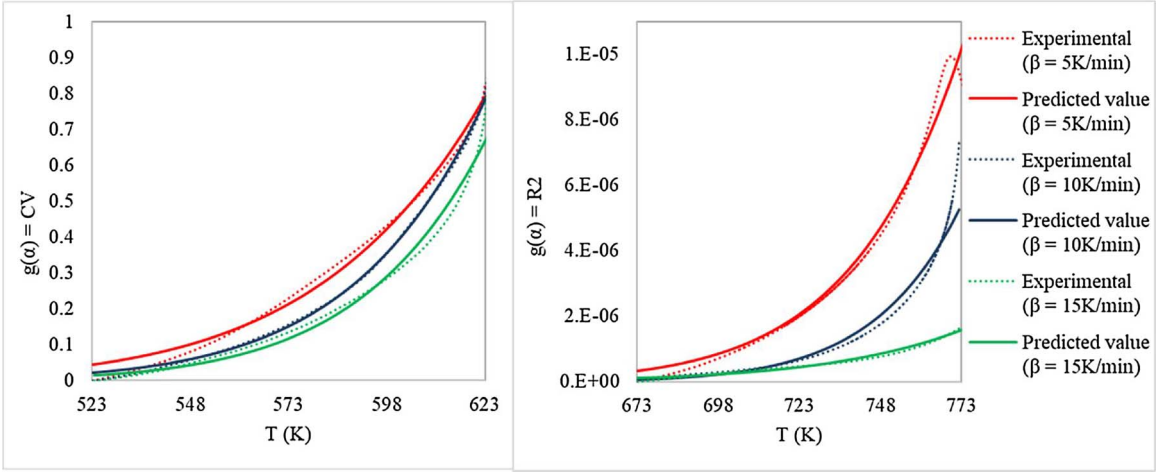

Fig. 11. Comparison of experimental and predicted values for marc at different heating rates by Coats-Redfern method for devolatilization and char combustion stages.

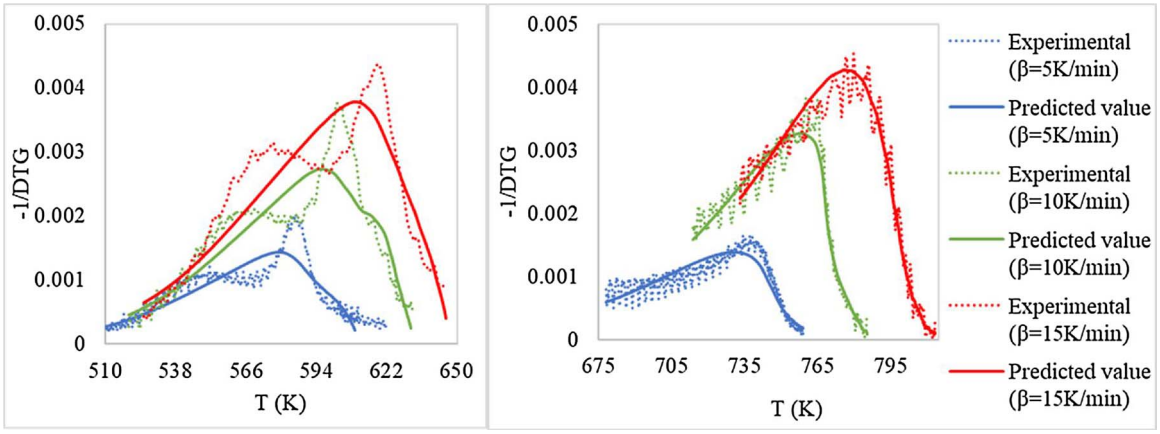

Fig. 12. Comparison of experimental and predicted values for peach pits at different heating rates by linear multiple regression method for devolatilization and char combustion stages.

Table 8
Activation energy obtained by the methods used.

Wastes	Kissinger	FWO	DAEM	RLM	CR
		Devolatilization stage			
Sawdust	92.99	133.56	131.15	64.83	102.85
Plum pits	59.14	110.69	103.76	39.50	95.43
Peach pits	90.64	117.17	113.83	66.61	96.04
Olive pits	116.92	109.58	106.12	52.20	91.58
Stalk	94.53	128.79	126.55	45.94	72.48
Marc	52.75	106.98	100.65	34.17	92.79
		Char combustion stage			
Sawdust	138.26	122.48	118.51	64.83	85.58
Plum pits	157.24	119.85	115.58	39.50	176.10
Peach pits	114.38	96.71	91.15	66.61	170.36
Olive pits	151.98	119.85	115.58	52.20	150.45
Stalk	82.82	154.88	120.58	45.94	123.66
Marc	65.39	112.02	106.38	34.17	151.50

respectively.

- The parameters obtained by Coats-Redfern method are the recommended for used in others studies. It is due to than is used a model for describe the reaction mechanism.
- The obtained thermodynamic parameters values, show that the lignocellulosic wastes decomposition under oxidative atmosphere has a low reaction favourability.

References

[1] C. Branca, C. Di Blasi, A unified mechanism of the combustion reactions of lignocellulosic fuels, Thermochim. Acta 565 (2013) 58–64, http://dx.doi.org/10.1016/j.tca.2013.04.014.

[2] A. Khawam, D.R. Flanagan, Solid-state kinetic models: basics and mathematical fundamentals, J. Phys. Chem. B 110 (2006) 17315–17328, http://dx.doi.org/10.1021/jp062746a.

[3] W.E. Brown, D. Dollimore, A.K. Galwey, Contributors to volume 22, Compr. Chem. Kinet. 22 (1980), http://dx.doi.org/10.1016/S0069-8040(08)70380-7.

[4] A.K. Burnham, R.L. Braun, Global kinetic analysis of complex materials, Energy Fuels 13 (1999) 1–22, http://dx.doi.org/10.1021/ef9800765.

[5] H.E. Kissinger, Reaction kinetics in differential thermal analysis, Anal. Chem. 29 (1957) 1702–1706, http://dx.doi.org/10.1021/ac60131a045.

[6] J.H. Flynn, The isoconversional method for determination of energy of activation at constant heating rates, J. Therm. Anal. 27 (1983) 95–102, http://dx.doi.org/10.1007/BF01907325.

[7] T. Ozawa, A new method of analyzing thermogravimetric data, Bull. Chem. Soc. Jpn. 38 (1965) 1881–1886, http://dx.doi.org/10.1246/bcsj.38.1881.

[8] A.I.-E.F. Karaosmanoglu, B.D. Cift, Determination of reaction kinetics of straw and stalk of rapeseed using thermogravimetric analysis, Energy Sources 23 (2001) 767–774, http://dx.doi.org/10.1080/009083101316862525.

[9] A. Garcia-Maraver, J.A. Perez-Jimenez, F. Serrano-Bernardo, M. Zamorano, Determination and comparison of combustion kinetics parameters ofagricultural biomass from olive trees, Renew. Energ. 83 (2015) 897–904, http://dx.doi.org/10.1016/j.renene.2015.05.049.

[10] B. Janković, L. Kolar-Anić, I. Smičiklas, S. Dimović, D. Arandelović, The non-isothermal thermogravimetric tests of animal bones combustion, Part. I. Kinetic Anal. Thermochim. Acta 495 (2009) 129–138, http://dx.doi.org/10.1016/j.tca.2009.06.016.

[11] A. Álvarez, C. Pizarro, R. García, J.L. Bueno, A.G. Lavín, Determination of kinetic parameters for biomass combustion, Bioresour. Technol. 216 (2016) 36–43, http://dx.doi.org/10.1016/j.biortech.2016.05.039.

[12] I. Abed, M. Paraschiv, K. Loubar, F. Zagrouba, M. Tazerout, Thermogravimetric investigation and thermal conversion kinetics of typical north african and, BioResources 7 (2012) 1200–1220.

[13] R. Volpe, J.M.B. Menendez, T.R. Reina, A. Messineo, M. Millan, Evolution of chars during slow pyrolysis of citrus waste, Fuel Process. Technol. 158 (2017) 255–263, http://dx.doi.org/10.1016/j.fuproc.2017.01.015.

[14] D.1102-84 ASTM, Standard Test Method for ash in wood, ASTM Int. 2 (2001), http://dx.doi.org/10.1520/D1894-14.2.

[15] E872–82 ASTM, Standard test method for volatile matter in the analysis of particulate wood fuels, ASTM Int. 14-16 (1998) E872–882, http://dx.doi.org/10.1520/E0872-82R06.2.

[16] C. Sheng, J.L.T. Azevedo, Estimating the higher heating value of biomass fuels from basic analysis data, Biomass Bioenergy 28 (2005) 499–507, http://dx.doi.org/10.1016/j.biombioe.2004.11.008.

[17] Y.S. Kim, Y.S. Kim, S.H. Kim, Investigation of thermodynamic parameters in the thermal decomposition of plastic waste-Waste lube oil compounds, Environ. Sci. Technol. 44 (2010) 5313–5317, http://dx.doi.org/10.1021/es101163e.

[18] A. Anca-Couce, A. Berger, N. Zobel, How to determine consistent biomass pyrolysis kinetics in a parallel reaction scheme, Fuel 123 (2014) 230–240, http://dx.doi.org/10.1016/j.fuel.2014.01.014.

[19] S. Ceylan, Y. Topçu, Pyrolysis kinetics of hazelnut husk using thermogravimetric analysis, Bioresour. Technol. 156 (2014) 182–188, http://dx.doi.org/10.1016/j.biortech.2014.01.040.

[20] J.H. Flynn, L.A. Wall, A quick, direct method for the determination of activation energy from thermogravimetric data, J. Polym. Sci. Part B 4 (1966) 323–328, http://dx.doi.org/10.1002/pol.1966.110040504.

[21] C.D. Doyle, Estimating isothermal life from thermogravimetric data, J. Appl. Polym. Sci. 6 (1962) 639–642, http://dx.doi.org/10.1002/app.1962.070062406.

[22] V. Vand, A theory of the irreversible electrical resistance changes of metallic films evaporated in vacuum, Proc. Phys. Soc. 55 (1943) 222.

[23] A. Bhavanam, R.C. Sastry, Kinetic study of solid waste pyrolysis using distributed activation energy model, Bioresour. Technol. 178 (2015) 126–131, http://dx.doi.org/10.1016/j.biortech.2014.10.028.

[24] A.W. Coats, J.P. Redfern, Kinetic parameters from thermogravimetric data, Nature 201 (1964) 68–69.

[25] L. Prasad, P.M.V. Subbarao, J.P. Subrahmanyam, Pyrolysis and gasification characteristics of Pongamia residue (de-oiled cake) using thermogravimetry and downdraft gasifier, Appl. Therm. Eng. 63 (2014) 379–386, http://dx.doi.org/10.1016/j.applthermaleng.2013.11.005.

[26] M. Valente, A. Brillard, C. Schönnenbeck, J.F. Brilhac, Investigation of grape marc combustion using thermogravimetric analysis. Kinetic modeling using an extended independent parallel reaction (EIPR), Fuel Process. Technol. 131 (2015) 297–303, http://dx.doi.org/10.1016/j.fuproc.2014.10.034.

[27] A. Bhavanam, R.C. Sastry, Kinetic study of solid waste pyrolysis using distributed activation energy model, Bioresour. Technol. 178 (2015) 126–131, http://dx.doi.org/10.1016/j.biortech.2014.10.028.

[28] A. Demirbas, Effects of temperature and particle size on bio-char yield from pyrolysis of agricultural residues, J. Anal. Appl. Pyrolysis 72 (2004) 243–248, http://dx.doi.org/10.1016/j.jaap.2004.07.003.

[29] G. Zheng, Thermal events occurring during the combustion of biomass residue, Fuel 79 (2000) 181–192, http://dx.doi.org/10.1016/S0016-2361(99)00130-1.

[30] B. Boonchom, Kinetic and thermodynamic studies of MgHPO4 · 3H2O by non-isothermal decomposition data, J. Therm. Anal. Calorim. 98 (2009) 863, http://dx.doi.org/10.1007/s10973-009-0108-2.

[31] I.T. Ahmed, Thermal decomposition study on mixed ligand thymine complexes of divalent nickel(II) with dianions of some dicarboxylic acids, J. Anal. Appl. Pyrolysis 80 (2007) 383–388, http://dx.doi.org/10.1016/j.jaap.2007.04.006.

[32] C.M. Santos, J. Dweck, R.S. Viotto, A.H. Rosa, L.C. de Morais, Application of orange peel waste in the production of solid biofuels and biosorbents, Bioresour. Technol. 196 (2015) 469–479, http://dx.doi.org/10.1016/j.biortech.2015.07.114.
[33] S. Vyazovkin, C.A. Wight, Model-free and model-fitting approaches to kinetic analysis of isothermal and nonisothermal data, Thermochim. Acta 340–341 (1999) 53–68, http://dx.doi.org/10.1016/S0040-6031(99)00253-1.
[34] A.O. Aboyade, T.J. Hugo, M. Carrier, E.L. Meyer, R. Stahl, J.H. Knoetze, J.F. G?rgens, Non-isothermal kinetic analysis of the devolatilization of corn cobs and sugar cane bagasse in an inert atmosphere, Thermochim. Acta 517 (2011) 81–89, http://dx.doi.org/10.1016/j.tca.2011.01.035.
[35] V.V. Boldyrev, Topochemistry of thermal decompositions of solids, Thermochim. Acta 100 (1986) 315–338, http://dx.doi.org/10.1016/0040-6031(86)87063-0.
[36] M. Amutio, G. Lopez, R. Aguado, M. Artetxe, J. Bilbao, M. Olazar, Kinetic study of lignocellulosic biomass oxidative pyrolysis, Fuel 95 (2012) 305–311, http://dx.doi.org/10.1016/j.fuel.2011.10.008.
[37] L. Sanchez-Silva, D. López-González, A.M. Garcia-Minguillan, J.L. Valverde, Pyrolysis, combustion and gasification characteristics of Nannochloropsis gaditana microalgae, Bioresour. Technol. 130 (2013) 321–331, http://dx.doi.org/10.1016/j.biortech.2012.12.002.